Available online at www.sciencedirect.com
SCIENCE DIRECT®
ELSEVIER
Chemical Physics Letters 408 (2005) 75–79
CHEMICAL PHYSICS LETTERS
www.elsevier.com/locate/cplett

A direct method to determine the chiral indices of carbon nanotubes

Zejian Liu [a], Lu-Chang Qin [a,b,*]

[a] Department of Physics and Astronomy, University of North Carolina at Chapel Hill, Campus Box 3255, Chapel Hill, NC 27599-3255, United States
[b] Curriculum in Applied and Materials Sciences, University of North Carolina at Chapel Hill, Chapel Hill, NC 27599-3255, United States

Received 15 March 2005; in final form 1 April 2005
Available online 25 April 2005

Abstract

A direct method is described to determine the chiral indices (u, v) of a carbon nanotube from a nanobeam electron diffraction pattern of the nanotube with high accuracy. This method is a one-step procedure and allows rapid and precise assignment of the chiral indices of carbon nanotubes. Using a contemporary electron microscope, we have been able to achieve an accuracy that enables us to assign the chiral indices unambiguously up to the range of (30, 30), corresponding to a diameter of 4.0 nm. Examples of determination of the chiral indices for two single-walled carbon nanotubes are presented as an illustration of the method.
© 2005 Elsevier B.V. All rights reserved.

1. Introduction

The atomic structure of a carbon nanotube can be described by its chiral indices (u, v) that define its perimeter vector (chiral vector) $\vec{A} = (u, v) = u\vec{a}_1 + v\vec{a}_2$, where $\vec{a}_1$ and $\vec{a}_2$ are the basis vectors of graphene with magnitude $a_1 = a_2 = a_0 = 0.2461$ nm and inter-angle 60° as schematically shown in Fig. 1a. The diameter d and helicity (chiral angle) α of the single-walled carbon nanotube are given by $d = (a_0/\pi)\sqrt{u^2 + v^2 + uv}$ and $\alpha = \cos^{-1}[(2u + v)/2\sqrt{u^2 + v^2 + uv}]$. An extraordinary property of carbon nanotubes is that, depending on its diameter and helicity, a carbon nanotube can be either metallic or semiconducting and, therefore, the determination and eventual control of the chiral indices are of vital importance to make carbon nanotubes useful in the envisaged nanoelectronic device applications. In terms of the chiral indices, when $u - v$ is divisible by 3, the nanotube is metallic [1,2]; otherwise it is semiconducting unless its diameter is extremely small when all nanotubes appear metallic [3].

It has been a challenge how to assign experimentally their chiral indices ever since the discovery of carbon nanotubes [4–6]. Many attempts have been devoted to the development of experimental methods for assigning the chiral indices and significant progress has been made using various analytical techniques including Raman spectroscopy [7,8], fluorescent spectroscopy [9,10], scanning probe microscopy [11,12] and electron diffraction [13–18]. The spectroscopic techniques have been able to provide an average measurement over a large number of nanotubes, but there is still no available technique that offers convenient, rapid and accurate determination of the atomic structure of individual carbon nanotubes.

Electron diffraction, especially nanobeam electron diffraction, has been a powerful technique in determining the atomic structure of carbon nanotubes. Here, we report a direct method to determine unambiguously the chiral indices (u, v) of a carbon nanotube that define its perimeter, therefore the diameter and helicity, from a nanobeam electron diffraction pattern of the nanotube with high accuracy. This method identifies the order of the Bessel function governing the intensities on the principal layer lines and is a one-step procedure to allow rapid and precise assignment of the chiral indices

* Corresponding author. Fax: +1 919 962 0480.
E-mail address: lcqin@physics.unc.edu (L.-C. Qin).

0009-2614/$ - see front matter © 2005 Elsevier B.V. All rights reserved.
doi:10.1016/j.cplett.2005.04.016

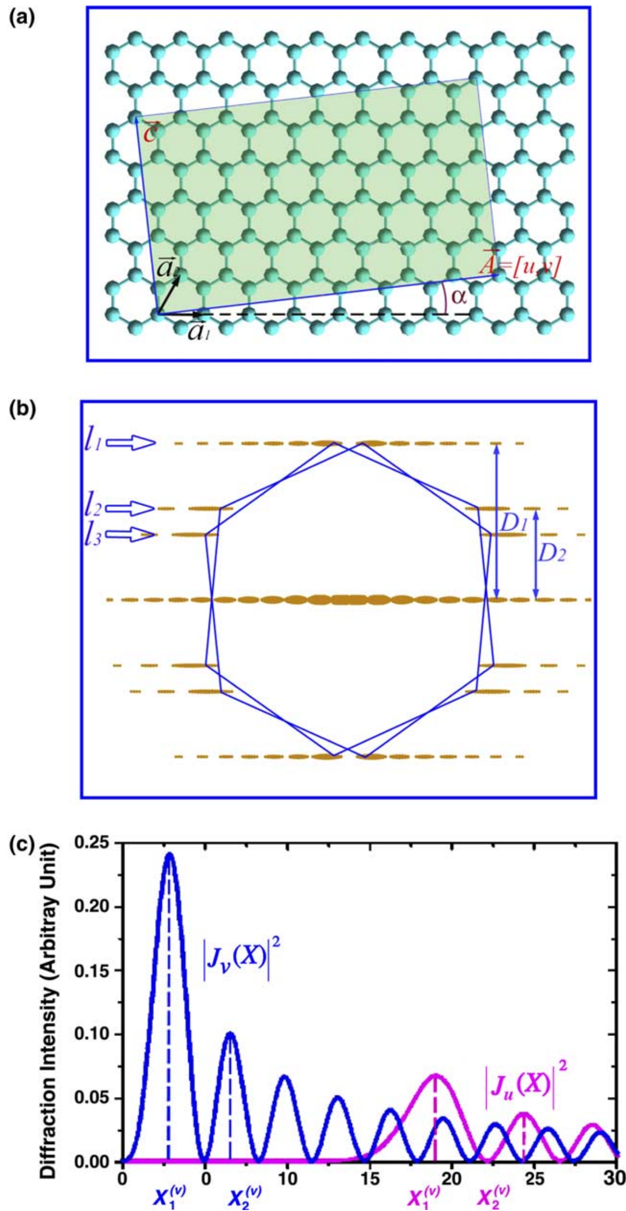

Fig. 1. (a) Schematic illustrating the chiral vector $\vec{A} = (u, v) = u\vec{a}_1 + v\vec{a}_2$ on graphene that defines the perimeter of a carbon nanotube. The rectangle shows projection of an asymmetric unit cell with dimensions A (perimeter) and c (axial periodicity). (b) Simulated electron diffraction pattern from single-walled carbon nanotube (17, 2). There are three principal layer lines above and below the equatorial line due to the principal reflections of graphene. Above the equatorial line, they are designated as principal layer lines l_1, l_2, and l_3, their intensities are proportional to $|J_v(\pi dR)|^2$ (blue line profile in (c)), $|J_u(\pi dR)|^2$ (pink line profile in (c)), and $|J_{u+v}(\pi dR)|^2$, respectively. (c) Ratios of the peak positions X_1 and X_2 on layer line l_1 (blue) and layer line l_2 (pink) are identifiers of the orders of the Bessel functions, v and u. (For interpretation of the references to color in this figure legend, the reader is referred to the web version of this article.)

of individual carbon nanotubes. Once the chiral indices of an isolated pristine carbon nanotube are obtained, its electronic behaviour, such as being metallic or semiconducting, can be identified immediately in experiment.

2. Theory

When an electron diffraction pattern from a single-walled carbon nanotube is formed, two sets of principal reflections are present in general, appearing as two twisted hexagonal patterns. One set is due to the top layer and the other due to the bottom layer, when the electron beam passes through the single-walled carbon nanotube. Since the nanotube is periodic in its axial direction, the scattering intensities show up on a set of equally spaced layer lines similar to the diffraction patterns obtained from DNA molecules [19,20]. The scattering intensity distribution on the layer line of index l can be calculated precisely from the analytic expression [21]

$$F(R, \Phi, l) = \sum_n B_n(R, \Phi) T_{nl}, \quad (1)$$

where

$$B_n(R, \Phi) = \exp[in(\Phi + \pi/2)] J_n(\pi\, dR) \quad (2)$$

describes the cylindrical curvature of the nanotube with $J_n(\pi dR)$ being the Bessel function of integer order n,

$$T_{nl} = \sum_j f_j \exp[2\pi i(nx_j/A) + lz_j/c] \quad (3)$$

expresses the planar structure factor of the nanotube in radial projection with unit cell dimensions A and c (Fig. 1a), respectively, f_j is the atomic scattering amplitude for atom located at (x_j, z_j) on the radial projection, the summation over j is done over all atoms in the asymmetric unit cell, and integer n is determined by the selection rule

$$l = [(u + 2v)n + 2(u^2 + v^2 + uv)m]/(uM) \quad (4)$$

satisfied by any and all possible integer values for m and M is the maximum common divisor of integers $u + 2v$ and $2u + v$. The intensity distribution on layer line l is $I(R, \Phi, l) = |F(R, \Phi, l)|^2$. A fortunate fact is that, even though the selection rule allows multiple orders of Bessel functions to contribute to a layer line, there is only one order of Bessel function that dominates the intensity distribution and all others have negligible contributions near the vertical axis passing through the origin.

Though the scattering intensities are observable on all layer lines, as illustrated schematically in Fig. 1b, the principal reflections of {1 0 0}* type bear the strongest intensities. These reflections give rise to three layer lines above and below the equatorial line, respectively. When the geometry of the electron diffraction pattern is considered, each layer line is governed by a single Bessel function of specific order that is related to the chiral indices of the nanotube [22]. If the three principal layer lines are designated as layers lines l_1, l_2, and l_3 as indicated in Fig. 1b,c, their intensities are related to the chiral indices u and v by

$$I_{l1}(R) \propto |J_v(\pi\, dR)|^2, \quad (5)$$

$$I_{l2}(R) \propto |J_u(\pi\, dR)|^2, \quad (6)$$

and

$$I_{l3}(R) \propto |J_{u+v}(\pi\, dR)|^2. \quad (7)$$

The layer line corresponding to the (1 1 0) reflections near the tubule axis has intensity distribution

$$I_{l4}(R) \propto |J_{u-v}(\pi\, dR)|^2. \quad (8)$$

The order n of Bessel function $J_n(X)$ can be determined by examining the positions of its peaks, which are unique to each Bessel function. An efficient and convenient means to determine the orders n of Bessel functions $J_n(X)$ is to examine the ratio X_2/X_1 of the positions of its first two peaks located at X_1 and X_2, respectively, or any other pair of peaks unique to this Bessel function. The measurement of X_1 and X_2 is schematically illustrated in Fig. 2c,d, from which the orders of Bessel functions, u and v, can be deduced directly. The chiral indices (u, v) can therefore be obtained directly by determining the orders of Bessel functions $J_v(X)$ and $J_u(X)$ with $X = \pi dR$ from the scattering intensity distribution on layer lines l_1 and l_2, whose intensities are proportional to $|J_v(\pi dR)|^2$ and $|J_u(\pi dR)|^2$, respectively. On the experimental diffraction pattern, the positions of the first two peaks, R_1 and R_2, can be measured and the ratio $R_2/R_1 = X_2/X_1$ is independent on the camera length of the electron microscope at which the electron diffraction pattern is acquired.

The method allows a rapid and accurate assignment of the chiral indices (u, v). From the ratios $R_2/R_1 = X_2/X_1$ measured directly from the electron diffraction pattern, the indices v and u can be obtained from the tabulated values given in Table 1. For Bessel functions $J_{18}(X)$ and $J_{19}(X)$, for example, the ratios of $X_2/X_1 = R_2/R_1$ are 1.266 and 1.256, respectively, and the difference is large enough to be identified unambiguously. Using our current method, we can obtain the peak positions with a precision of 0.3%, which allows us to assign the chiral indices unambiguously up to index 30 or nanotube diameter up to 4 nm.

For non-helical nanotubes, i.e., zigzag and armchair nanotubes with crystallographic indices $(u,0)$ and (u, u), respectively, overlap of the principal layer lines occurs. For a zigzag nanotube of indices $(u,0)$, layer lines l_2 and l_3 overlap with each other and its first principal layer line (l_1) has intensity distribution proportional to $|J_0(\pi dR)|^2$ and the second layer line (l_2) has intensity proportional to $|J_u(\pi dR)|^2$. For an armchair nanotube (u, u), the first layer line l_1 and the second line l_2 overlap with intensities proportional to $|J_u(\pi dR)|^2$ and layer line l_3 falls on the equatorial line.

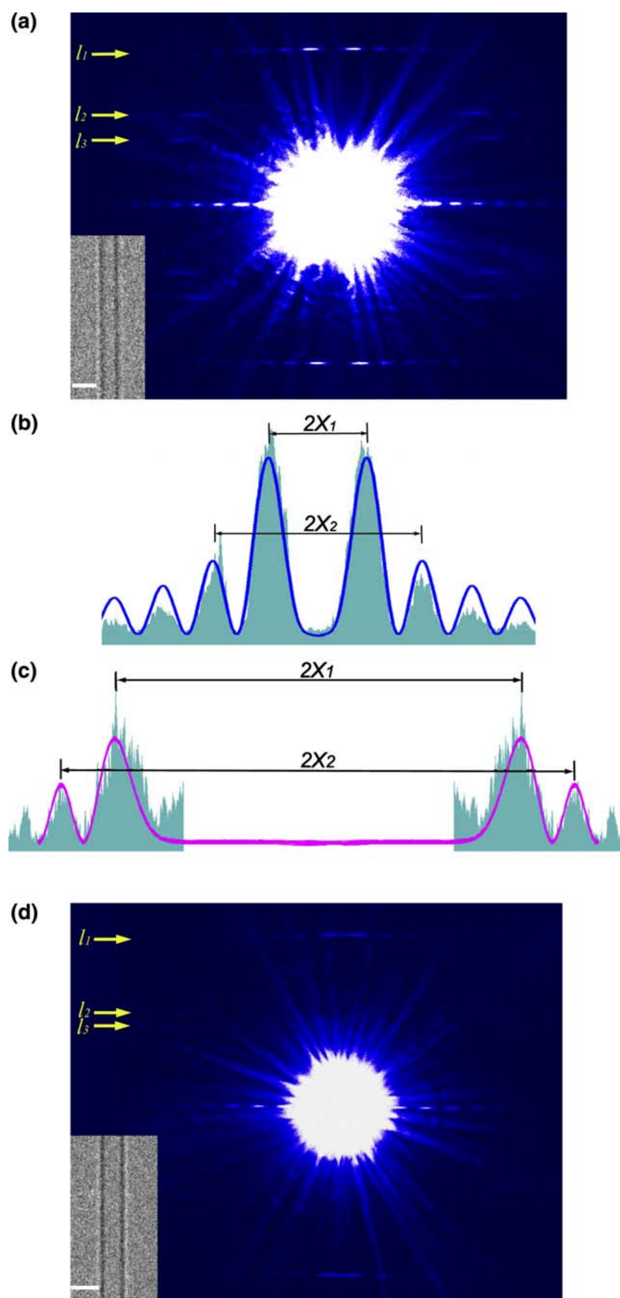

Fig. 2. (a) Nanobeam electron diffraction pattern taken at 80 kV of a single-walled carbon nanotube of diameter 1.4 nm, whose electron microscope image is shown as inset (scale bar: 2 nm). The chiral indices were determined to be (17,2) from the intensity profiles of layer lines l_1 and l_2 using the ratio of its first two peak positions X_2/X_1 as shown in (b) and (c), respectively. It is a metallic nanotube of diameter d = 1.416 nm and helicity α = 5.50°. (d) Nanobeam electron diffraction pattern of a nanotube (TEM image given in inset; scale bar: 2 nm) of similar diameter 1.4 nm. Its chiral indices were determined to be (17,1), which is a semiconducting nanotube with diameter 1.372 nm and helicity 2.83°.

3. Examples of application

We have employed this method to determine the chiral indices of single-walled carbon nanotubes produced by arc-discharge [23]. In order to minimize radiation damage to the carbon nanotubes, we operated the transmission electron microscope (JEM 2010F equipped with a field-emission gun) at 80 kV. Nanobeam electron

Table 1
Ratio of positions of the first two peaks, X_2/X_1, of Bessel function $J_n(X)$ for order $n = 1$ to $n = 30$

n	X_2/X_1
1	2.892
2	2.197
3	1.907
4	1.751
5	1.639
6	1.565
7	1.507
8	1.465
9	1.428
10	1.398
11	1.373
12	1.350
13	1.332
14	1.315
15	1.301
16	1.287
17	1.275
18	1.266
19	1.256
20	1.247
21	1.239
22	1.232
23	1.226
24	1.218
25	1.211
26	1.206
27	1.201
28	1.196
29	1.192
30	1.188

The order n of the Bessel function can be identified from the characteristic value X_2/X_1 that is unique to each Bessel function.

diffraction patterns were acquired with a parallel beam of 20-nm spot size obtained with a 10-μm condenser aperture and exciting the first condenser lens to maximum. The nanobeam electron diffraction patterns were recorded on photographic films, which were later scanned digitally to acquire more accurate measurement of the intensity distribution on the concerned layer lines. Fig. 2a shows a nanobeam electron diffraction pattern of a single-walled carbon nanotube of diameter about 1.4 nm (high-resolution electron microscope image is given as inset with 2-nm scale bar). From the intensity profiles on the three principal layer lines (l_1, l_2, and l_3), the ratios $R_2/R_1 = X_2/X_1$ on layer lines l_1 and l_2 (Fig. 2b,c) were measured to be 2.200, and 1.279, respectively. The orders of Bessel functions, and thus the chiral indices of the nanotube, were determined to be $v = 2$, and $u = 17$ (cf. Table 1). Nanotube (17,2) is a metallic nanotube of diameter 1.416 nm and helicity 5.50°. Fig. 2d shows the electron diffraction pattern obtained from another nanotube of similar diameter (image shown as inset with scale bar 2 nm). Using the same method, the chiral indices for this single-walled carbon nanotube were determined to be (17,1), which is a semiconducting tubule of diameter 1.372 nm and helicity 2.83°.

When the diameter of the nanotube is large, the ratio of X_2 and X_1 for a Bessel function is closer to that of its neighbors. In this case, layer line l_3 can be used as supplementary information to narrow down the choices and minimize the possible errors. Another useful relationship that can serve the same purpose is

$$v/u = (2D_2 - D_1)/(2D_1 - D_2), \quad (9)$$

where D_1 and D_2 are the spacings from the equatorial line to layer lines l_1 and l_2, respectively, as depicted in Fig. 1b.

The major sources of error of the present method are from: (a) low signal/noise ratio due to the small number of atoms in the carbon nanotube and (b) the identification of the peak positions in the intensity distribution on the principal layer lines. The signal/noise ratio can be enhanced by applying longer exposure in acquiring the experimental electron diffraction pattern. Before higher-resolution CCD cameras become available for acquiring the electron diffraction patterns directly in the electron microscope, using a high-resolution scanner to digitize the diffraction intensity data recorded on photographic films still offers the best data. The ultimate resolution for this case is limited by the optical resolution of the recording film.

This approach can also be applied to the study of multiwalled carbon nanotubes [24]. However, cautions must be exercised when there is an overlap of layer lines from different shells of the same helicity, in which the oscillations on this particular layer line may be dominated by more than one Bessel function [25].

4. Conclusions

We have described a direct method that allows rapid and accurate determination of the chiral indices (u, v) of carbon nanotubes from an electron diffraction pattern. The electron diffraction intensities on the three principal layer lines corresponding to the graphite (1 0 0) reflections are $|J_v(\pi dR)|^2$, $|J_u(\pi dR)|^2$, and $|J_{u+v}(\pi dR)|^2$, respectively. By determining the order of the Bessel function that governs the layer line intensity distribution, the chiral indices (u, v) can be obtained unambiguously.

References

[1] N. Hamada, S. Sawada, A. Oshiyama, Phys. Rev. Lett. 68 (1992) 1579.
[2] R. Saito, M. Fujita, G. Dresselhaus, M.S. Dresselhaus, Appl. Phys. Lett. 60 (1992) 2204.
[3] L.-C. Qin, X. Zhao, K. Hirahara, Y. Miyamoto, Y. Ando, S. Iijima, Nature (London) 408 (2000) 50.
[4] S. Iijima, Nature (London) 354 (1991) 56.
[5] S. Iijima, T. Ichihashi, Nature (London) 363 (1993) 603.

[6] D.S. Bethune, C.H. Kiang, M.S. De Vries, G. Gorman, R. Savoy, J. Vazquez, R. Beyers, Nature (London) 363 (1993) 605.
[7] A.M. Rao, E. Richter, S. Bandow, B. Chase, P.C. Eklund, K.A. Williams, S. Fang, K.R. Subbaswamy, M. Menon, A. Thess, R.E. Smalley, G. Dresselhaus, M.S. Dresselhaus, Science 275 (1997) 187.
[8] A. Jorio, M.A. Pimenta, A.G. Souza, R. Saito, G. Dresselhaus, M.S. Dresselhaus, New J. Phys. 5 (2003) 139.
[9] S.M. Bachilo, M.S. Strano, C. Kittrell, R.H. Hauge, R.E. Smalley, R.B. Weisman, Science 298 (2002) 2361.
[10] M.S. Strano, S.K. Doorn, E.H. Haroz, C. Kittrell, R.H. Hauge, R.E. Smalley, Nano Lett. 3 (2003) 1091.
[11] J.W.G. Wildoer, L.C. Venema, A.G. Rinzler, R.E. Smalley, C. Dekker, Nature (London) 391 (1998) 59.
[12] T.W. Odom, J.-L. Huang, P. Kim, C.M. Lieber, Nature (London) 391 (1998) 62.
[13] L.-C. Qin, T. Ichihashi, S. Iijima, Ultramicroscopy 67 (1997) 181.
[14] J.M. Cowley, P. Nikolaev, A. Thess, R.E. Smalley, Chem. Phys. Lett. 265 (1997) 379.
[15] L.-C. Qin, S. Iijima, H. Kataura, Y. Maniwa, S. Suzuki, Y. Achiba, Chem. Phys. Lett. 268 (1997) 101.
[16] M. Kociak, K. Suenaga, K. Hirahara, Y. Saito, T. Nakahira, S. Iijima, Phys. Rev. Lett. 89 (2002) 155501.
[17] M. Kociak, K. Hirahara, K. Suenaga, S. Iijima, Eur. Phys. J. B 32 (2003) 457.
[18] J.M. Zuo, I. Vartanyants, M. Gao, R. Zhang, L.A. Nagahara, Science 300 (2003) 1419.
[19] M.H.F. Wilkins, A.R. Stokes, H.R. Wilson, Nature (London) 171 (1953) 738.
[20] R.E. Franklin, R.G. Gosling, Nature (London) 171 (1953) 739.
[21] L.-C. Qin, J. Mater. Res. 9 (1994) 2450.
[22] L.-C. Qin, Chem. Phys. Lett. 297 (1998) 23.
[23] C. Journet, W.K. Maser, P. Bernier, A. Loiseau, M. Lamy de la Chapelle, S. Lefrant, P. Deniard, R. Lee, J.E. Fischer, Nature (London) 388 (1997) 756.
[24] Z. Liu, Q. Zhang, L.-C. Qin, Appl. Phys. Lett., 2005 (in press).
[25] Z. Liu, L.-C. Qin, Chem. Phys. Lett. 402 (2005) 202.